Title

Sustained, localized salicylic acid delivery enhances diabetic bone regeneration via prolonged mitigation of inflammation

Journal

Journal of Biomedical Materials Research Part A, 104(10)

ISSN

1549-3296

Authors

Yu, Weiling
Bien-Aime, Stephan
Mattos, Marcelo
et al.

Publication Date

2016-10-01

DOI

10.1002/jbm.a.35781

Peer reviewed

HHS Public Access

Author manuscript

J Biomed Mater Res A. Author manuscript; available in PMC 2020 November 21.

Published in final edited form as:

J Biomed Mater Res A. 2016 October ; 104(10): 2595–2603. doi:10.1002/jbm.a.35781.

Sustained, localized salicylic acid delivery enhances diabetic bone regeneration via prolonged mitigation of inflammation

Weiling Yu[1], **Stephan Bien-Aime**[2], **Marcelo Mattos**[3], **Sarah Alsadun**[3], **Keisuke Wada**[3], **Sarah Rogado**[4], **Joseph Fiorellini**[3], **Dana Graves**[3,*], **Kathryn Uhrich**[1,2,*]

[1]Department of Biomedical Engineering, Rutgers, the State University of New Jersey, 599 Taylor Road, Piscataway, New Jersey

[2]Department of Chemistry and Chemical Biology, Rutgers, the State University of New Jersey, 610 Taylor Road, Piscataway, New Jersey

[3]Department of Periodontics, University of Pennsylvania School of Dental Medicine, 240 South 40th Street, Philadelphia, Pennsylvania

[4]Department of Pharmaceutics, Ernest Mario School of Pharmacy, Rutgers, the State University of New Jersey, 610 Taylor Road, Piscataway, New Jersey

Abstract

Diabetes is a metabolic disorder caused by insulin resistance and/or deficiency and impairs bone quality and bone healing due to altered gene expression, reduced vascularization, and prolonged inflammation. No effective treatments for diabetic bone healing are currently available, and most existing treatments do not directly address the diabetic complications that impair bone healing. We recently demonstrated that sustained and localized delivery of salicylic acid (SA) via an SA-based polymer provides a low-cost approach to enhance diabetic bone regeneration. Herein, we report mechanistic studies that delve into the biological action and local pharmacokinetics of SA-releasing polymers shown to enhance diabetic bone regeneration. The results suggest that low SA concentrations were locally maintained at the bone defect site for more than 1 month. As a result of the sustained SA release, a significantly reduced inflammation was observed in diabetic animals, which in turn, yielded reduced osteoclast density and activity, as well as increased osteoblastogenesis. Based upon these results, localized and sustained SA delivery from the SA-based polymer effectively improved bone regeneration in diabetic animals by affecting both osteoclasts and osteoblasts, thereby providing a positive basis for clinical treatments.

Keywords

diabetic bone healing; control inflammation; salicylic acid; controlled and sustained drug delivery; histology

Correspondence to: K. Uhrich; keuhrich@rutgers.edu.

*These authors contributed equally as senior authors of this study.

Additional Supporting Information may be found in the online version of this article.

INTRODUCTION

Diabetes is a metabolic disorder caused by insulin resistance and/or deficiency that affected nearly 10% of the US population in 2012.[1] If the current trend continues, the diabetic population is expected to expand to one-third of the US adult population by 2050.[2] Thus, the sequelae associated with diabetes will become increasingly significant over the next few decades. A major complication of diabetes is impaired bone quality and bone healing capability, which is caused by diminished vascularity, decreased gene expression levels required to regenerate bone, increased systemic inflammation, and prolonged inflammatory response to injury.[3,4] Plausible causes for impaired bone healing in diabetics include prolonged osteoclastogenesis, loss of mesenchymal stem cells and reduced capacity to form bone.[5–7]

The current “gold standard” to treat orthopedic and oral-facial defects is bone grafting, which does not address the underlying diabetic complications. Diabetic subjects under these treatments therefore suffer from a greater degree of variability in treatment outcomes and increased infection rates.[8,9] Although studies have demonstrated that growth factors such as bone morphogenic proteins (BMP) are beneficial for bone regeneration in humans,[10] these proteins are extremely expensive and have unresolved safety concerns. For example, high complication rates and potential carcinogenicity of BMPs in humans are known: the BMP signaling pathway leads to enhanced proliferation in serous ovarian cancer—a potential therapeutic target.[11,12] With the rapidly expanding diabetic population and the lack of effective diabetic bone healing options, treatments that target the osteogenesis-impairing diabetic complications meet a critical need.

In previous work we demonstrated that a low-cost, local and sustained delivery of salicylic acid (SA) via a SA-based poly(anhydride ester) (SAPAE) significantly enhanced bone regeneration in diabetic rats based on micro-CT analysis and confirmation by histology.[13] The relative ratio of bone regeneration with SAPAE treatment versus control (i.e., without SAPAE treatment) is shown in Table I. In the rat mandibular bone defect model, the amount of new bone formed was easily determined as the defect was originally empty and thus bone measured within the original defect was the result of new bone formation. SAPAE had a greater effect on stimulating new bone formation in the diabetic than the normal as shown at the 12-week time point in Table I ($P < 0.05$). SAPAE contains chemically incorporated SA in its backbone and can gradually release SA via hydrolysis (Fig. 1). This offers an exceedingly high SA loading (~70%) compared to < 30% loadings from physical incorporation.[14] The SAPAE degradation mechanism is primarily surface erosion and yields a near zero-order release profile, meaning that the SA release rate is relatively constant and delivery is predictable.[15] The duration of SA release from SAPAE can last from weeks to months, making it an ideal material to target chronic conditions, such as diabetic bone healing.[15] SA is a well-known nonsteroidal anti-inflammatory drug that suppresses the activation of nuclear factor kappa-light-chain-enhancer of activated B cells (NF-κB).[16] NF-κB is involved in the production of proinflammatory cytokines, such as tumor necrosis factor (TNF)-α, interleukin (IL)–1 and IL-6, which can increase bone resorption and reduce bone formation, especially in diabetic subjects.[17–20] It is hypothesized that the prolonged

suppression of the aforementioned proinflammatory cytokines by SA might therefore increase diabetic bone regeneration.[13]

Our previous work showed the positive effects of SA on enhancing bone regeneration in diabetic rats,[13] yet the mechanistic basis was not identified; this aspect is crucial to identify treatment options. This study investigates the local pharmacokinetics of SAPAE using an *in vitro* agar-based model, histologically assesses local inflammation levels as well as the behaviors of osteoclasts and osteoblasts. SAPAE significantly increased osteoblastogenesis, reduced local inflammation and osteoclastogenesis in diabetic rats. As the application of SAPAE for diabetic bone is novel and shows promising results, the mechanistic study presented herein sets an important and valuable reference for future translation of this novel application.

MATERIALS AND METHODS

Sample preparation

SAPAE was synthesized using previously reported methods.[21] The polymer was ground into a fine powder and physically mixed with freeze-dried bone allograft (LifeNet Health®, Virginia Beach, VA) at a 1:1 weight ratio (7.5 mg of SA-PAE mixed with 7.5 mg of bone graft). Approximately 40 μL light mineral oil (Sigma–Aldrich, Milwaukee, WI) was added to the mixture, which was then sterilized under ultra-violet light in a Spectrolinker XL-1500 UV Crosslinker (Spectronics Corporation, Westbury, NY) at λ = 254 nm and 5500–6500 μW cm^{-2} for 900 s. Control samples were prepared without SAPAE and treated identically to the SAPAE-containing samples.

Animal study

A rat mandibular defect model was used and surgery details were presented in the previous publication.[13] Animal care and surgical procedures were approved by the IACUC of the University of Pennsylvania (Philadelphia, PA). Fifty-six adult male Sprague–Dawley rats weighing 250–350 g were used, n = 7 per group. The rats were randomly divided into diabetic and normoglycemic groups. Diabetes was induced by intraperitoneal injection of streptozotocin, 70 mg kg^{-1} (Sigma–Aldrich, Milwaukee, WI). Blood glucose was monitored by the glucose-oxidase method (Glucometer Encore, Miles, Elkhart, IN) and HbA1c was measured at the time of euthanasia. A blood glucose level >250 mg dL^{-1} was considered diabetic. Animals were monitored for 3 weeks to confirm their diabetic status and to evaluate their daily food intake, activity, weight, and overall health. Of the 56 rats that underwent surgery, two died during the procedure; no significant reductions in body weight occurred and three postoperative infections were observed in the diabetic group.

All procedures were performed under general anesthesia with an intraperitoneal injection of ketamine, 75 mg kg^{-1} (Fort Dodge Laboratories, Fort Dodge, IA) and xylazine, 5 mg kg^{-1} (Miles, Shawnee Mission, KS). Surgical procedures were performed under sterile conditions. A 15- to 20-mm incision was made on the lateral aspect of the mandible. A 5-mm diameter osteotomy defect was created at the angle of the mandible using a trephine burr with sterile saline irrigation. The site was grafted with SAPAE/graft mixture or bone

graft alone as prepared in Sample Preparation section. A BioGuide® resorbable collagen membrane (Geistlich Pharma., North America, NJ) was adapted to circumferentially cover the defect. The surgical field was closed in layers; a muscular layer and the external skin layer, using Chromic gut 5–0 resorbable sutures (Ethicon, Somerville, NJ). A single dose of buprenorphine (0.05 mg kg^{-1}) was administered for postoperative pain relief. Rats were euthanized at 4 and 12 weeks. The mandibles were dissected and fixed in 4% phosphate buffered formalin solution for 24 h and then stored in PBS until microcomputed tomography (micro-CT) scans were performed. Results of micro-CT have been previously published[13] and summarized in Table I.

In vitro release study in agar that mimics physiological conditions

Sample preparation.—Agar-based systems were formulated to mimic the *in vivo* physical environment for SAPAE degradation (Fig. 2). A plastic sheet (polystyrene, 0.55 mm thickness, LifeNet Health®, Virginia Beach, VA) was punched to form a 5-mm circular aperture to mimic the mandibular bone defect described above. SAPAE, bone allograft (LifeNet Health®, Virginia Beach, VA) and light mineral oil, with the same quantities in the animal study above (Sample Preparation section), were placed in the plastic aperture. Agar (0.015 g mL^{-1}, Sigma–Aldrich, Milwaukee, WI) was used to surround and seal the plastic sheet to mimic the soft tissues surrounding the mandibular bone defect.

Release study.—Each system was submerged in 50-mL phosphate buffered saline (PBS, pH 7.4) (Sigma–Aldrich, Milwaukee, WI) in a controlled environment incubator-shaker (New Brunswick Scientific, Edison, NJ) at 60 rpm at 37°C to mimic physiological conditions. At predetermined time points, agar systems were cut open along the midline and rinsed with 15 mL of PBS; this SA quantity should represent the local SA concentration at the bone defect. Media containing the recovered SA was then analyzed by an Perkin Elmer Lambda XLS spectrophotometer (Waltham, MA) at λ = 303 nm, the maximum absorption wavelength for SA at which all other SAPAE degradation products minimally absorb.[15] SA concentrations were calculated based on a calibration curve of absorbance from solutions prepared with known SA concentrations. Before the cut-open time, 50 mL of the surrounding release media was removed every other day and replenished with 50 mL fresh PBS to ensure sink conditions. The spent release media was also analyzed for SA concentration, representing systemic SA concentrations. This study was performed in triplicate for each time point.

Tissue processing

Mandibular bone was dissected after animal euthanasia, fixed in 4% phosphate buffered formalin solution for 24 h, decalcified in 10% EDTA (Fisher scientific USA, Pittsburgh, PA), embedded in low melting paraffin (Leica Biosystems, Richmond, IL), and sectioned at 5 μm (HM355, Thermo Scientific, Waltham, MA) at the defect midline.

Selection of regions-of-interest (area of new bone formation)

Hematoxylin and eosin (H&E) staining (Sigma–Aldrich, Saint Louis, MO) was performed. The defect boundary position was identified based on the differing patterns of old bone and the newly formed bone. Specifically, older bone generally has a laminar pattrn, whereas

newer bone is less well organized. A 2.5-mm length rectangle (representing half of the 5 mm defect) was then drawn to define the area of new bone formation (Supporting Information Fig. S1). Images were taken with a Motic BA210 microscope and analyzed using Motic Image Plus 2.0 (Motic, British Columbia, Canada).

Inflammation assessment

Quantification of polymorphonuclear cells (PMNs) and mononuclear cells (MNCs).—Specimens from 4-week treatments were chosen for inflammation analysis since it reflects a period of active bone remodeling in this animal model and the inflammation level at this time affects bone formation more directly.[22] In addition, it is well established that the primary inflammatory defect in bone associated with diabetes has prolonged, rather than acute, inflammation and affects bone formation at this time point.[23,24] For these reasons, 4-week time point specimens were chosen to evaluate post-injury inflammation in diabetic animals. The presence of PMNs and MNCs reflect the overall level of inflammation and can be distinguished from other cell types based on their unique nuclear structure. PMNs were identified by their horse-shoe shaped nucleus and MNCs identified by their round and evenly dark nucleus. Approximately 4–10 representative fields evenly spaced in the area of new bone formation were examined to quantify PMNs and mononuclear cells expressed as the number per mm. The analysis excluded bone matrix, surrounding muscle, adipose tissue and hematopoietic tissue. Images were taken with 60× objective of a Motic BA120 microscope and analyzed using Motic Image Plus 2.0 (Motic, British Columbia, Canada). $N = 5–8$ for each treatment group.

Immunofluorescence staining against IL-1α.—Slides were deparaffinized and antigen retrieved in citrate buffer (pH 6) (Sigma, Saint Louis, MO) in a pressure cooker (2100 retriever, Aptum Biologics, Southampton, UK) (121°C) for 30 min. Slides were incubated with primary antibody (goat anti-IL-1α, 1:200 dilution, R&D systems AF-400-NA, Minneapolis, MN) overnight at 4°C, with same concentrations of goat IgG and a nonspecific peptide as negative controls. Slides were then incubated with secondary antibody (donkey-anti-goat IgG, 1:1000 dilution Jackson Immunoresearch, West Grove, PA). Tyramide signal amplification (PerkinElmer, Waltham, MA) was used to enhance the chromogenic signal. Mean fluorescence intensity in two to three representative areas within the area of new bone formation were measured excluding areas of bone, bone allograft, muscle, adipose tissue, and hematopoietic tissue. Mean fluorescence intensity was normalized against the value of negative control slides for final analysis. Images were taken with 20× objective of a Nikon Eclipse 90i microscope (Nikon, Melville, NY) and analyzed using NIS Elements-AR software (Nikon). $N = 4–6$ for each treatment group.

Osteoblast analysis

A standard method was used to assess the number of bone-lining osteoblasts. Osteoblasts were identified by their cuboid morphology and their location, lining the bone edge (Supporting Information Fig. S2).[25] The number of bone-lining osteoblasts within the area of new bone formation were quantified and normalized by the length of bone to calculate osteoblast density. The length of bone covered by osteoblasts was also quantified and normalized by total bone length in area of new bone formation to calculate the percentage of

bone that is undergoing bone formation. Images were taken with 60× objective of Motic BA120 microscope and analyzed using Motic Image Plus 2.0 (Motic, British Columbia, Canada). As osteoblasts cannot be clearly distinguished at lower power, only a high power representative image is shown. $N = 5–8$ for each treatment group.

Osteoclast staining and analysis

Osteoclasts were identified as multinucleated cells lining bone that also tested positive for tartrate-resistance acid phosphatase (TRAP) staining or expression of cathepsin-K, as determined by immunohistochemistry. For TRAP staining, slides were deparaffinized and stained using the acid phosphatase, leukocyte TRAP kit (Sigma–Aldrich, St. Louis, MO) following manufacturer's protocol. For cathepsin-K immunohistochemistry staining, slides were deparaffinized and antigen retrieved in citrate buffer (pH 6) for 12 minutes at 98°C. Slides were then incubated with primary antibody overnight at 4°C (rabbit polyclonal to cathepsin K, 1:5000 dilution, Abcam-ab19027, Cambridge, MA) with rabbit IgG under the same concentration as negative control. The slides were then incubated with secondary antibody (goat anti-rabbit IgG, EMD Millipore, Billerica, MA). Tyramide signal amplification (PerkinElmer, Waltham, MA) was used to enhance the chromogenic signal. Positively stained cells with multiple nuclei were identified as osteoclasts. The number of bone-lining osteoclasts within area of new bone formation were quantified and normalized by the length of bone edge to calculate osteoclast density. Lacunae length was also measured and normalized by total bone length within area of new bone formation to calculate the percentage of bone surface that is undergoing bone resorption, which reflects osteoclast activity. Images were taken with 10× and 40× objective of Motic microscope and analyzed using Motic Image Plus 2.0 (Motic, British Columbia, Canada). $N = 5–8$ for each treatment group.

Statistical analysis

The difference among groups at each time point was analyzed by one-way ANOVA with Tukey's *post hoc* test. Significance was determined at $P < 0.05$.

RESULTS

In vitro release study

Based upon previous studies, the local SA release profile at the defect site is important for bone healing. To understand the local SAPAE pharmacokinetics without sacrificing an overly high number of animals, agar-based systems were developed to mimic the physical conditions in animals as described in *In Vitro* Release Study in Agar That Mimics Physiological Conditions Section. Release curves of local SA concentration in the plastic aperture (representing bone defect site) displayed a three-phase profile: relatively low values before day 2 (lag period), peaking at day 3–6, then a slowed SA release [Fig. 3(A)]. SA concentration in the bulk PBS (representing systemic SA concentrations) showed an initial lag period for 2 days, followed by a rapid and constant release at day 3–7, and then a slow and steady release [Fig. 3(B)]. Total daily SA release (SA released in plastic aperture plus in PBS) is shown in Figure 3(C). At the end of the study (31 days), 60% of the total SA

incorporated in SAPAE was released and the remaining 40% was still in the polymer or entrapped by agar.

Inflammation assessment

To assess local inflammation, inflammatory cells in the area of new bone formation, specifically polymorphonuclear leukocytes and mononuclear cells, which consist largely of monocytes/macrophages, were quantified. Inflammatory marker IL-1α was also measured to provide molecular-level information as detailed below. Four-week post-operation samples were chosen for inflammation analysis because inflammation during this period directly affects bone formation.[23] Although may be considered a late time point in normal subjects, it is relevant for diabetic subjects; the inflammatory responses in diabetic bone defects are prolonged rather than acute, and present at 4 weeks.[24] For these reasons we focused on a 4-week time point rather than an earlier time point (e.g., 3 days post-operation) for the analysis.[23,26]

PMN and mononuclear cell quantification.—Cells with horse-shoe shaped nucleus were identified as PMN and cells with round and evenly dark nucleus were identified as MNC (Fig. 4). Diabetic rats without SAPAE treatment had a significantly greater PMN/mononuclear cell infiltrate in healing bone compared to their normoglycemic counterpart ($P < 0.05$, Fig. 5). SAPAE significantly reduced this cellular infiltrate in both diabetic and normal rats ($P < 0.05$) with a greater change observed in the diabetic group. SAPAE treatment brought the infiltration level in diabetic animals to that of the normoglycemic animals (i.e., compare “normal + SAPAE” with “diabetic + SAPAE”).

IL-1α analysis.—IL-1α was measured by quantitative immunofluorescence based on the mean fluorescent intensity analysis. Diabetic animals receiving SAPAE had significantly lower IL-1α mean fluorescent intensity in the area of new bone formation ($P < 0.05$), indicating that SAPAE significantly reduced local inflammation in diabetic animals (Fig. 6). After SAPAE treatment, IL-1α levels in the diabetic group were equivalent to the normoglycemic.

Bone resorption assessment

Bone lining osteoclasts within the defect region were identified (Fig. 7) and their density and activity were analyzed. Since bone remodeling between 4 and 12 weeks, we examined specimens 4 and 12-weeks post-operation. At 4 weeks, both diabetic and normal rats receiving SAPAE had significantly lower osteoclast density compared to their non-SAPAE counterparts ($P < 0.05$, Fig. 8, left). At 12 weeks, SAPAE significantly reduced osteoclastogenesis in diabetic rats ($P < 0.05$) while the effect on normal rats was not statistically significant ($P > 0.05$, Fig. 8, left). At both time points, SAPAE reduced diabetic osteoclasts density to the normoglycemic level; and diabetic rats without SAPAE had higher osteoclast density than their normal counterparts.

The osteoclast activity analysis showed similar trends. Diabetes significantly increased osteoclast activity at 4 weeks (cf. “Normal + non-SAPAE” with “Diabetic + non-SAPAE”) ($P < 0.05$). SAPAE significantly reduced osteoclast activity (indicated by the percentage of

bone surface covered by lacunae) in both normal and diabetic rats at 4 weeks ($P < 0.05$) and in diabetic but not normoglycemic rats at 12 weeks ($P > 0.05$, Fig. 8, right). Diabetic osteoclast activity was normalized by SAPAE at 4 and 12 weeks.

Bone formation assessment

Diabetes significantly reduced osteoblast density at 4 and 12 weeks when no SAPAE was administered ($P < 0.05$). Diabetic rats receiving SAPAE exhibited significantly higher osteoblast density, which reflects higher osteoblastogenesis, compared to their non-SAPAE counterparts at 4 and 12 weeks (Fig. 9, left). SAPAE slightly increased osteoblast density in normal rats at 4 weeks, but the difference was not statistically significant. A similar pattern was observed for the analysis of bone forming area (Fig. 9, right). Diabetes significantly reduced this value at 4 and 12 weeks when no SAPAE was administered ($P < 0.05$). Diabetic rats receiving SAPAE treatments had significantly higher percentage of bone that was covered by osteoblasts and undergoing bone formation at 4 and 12 weeks ($P < 0.05$). SAPAE did not significantly increase this value in normal rats ($P > 0.05$).

DISCUSSION

It was previously established that SAPAE significantly enhanced diabetic bone regeneration at 4 and 12 weeks in rat mandibular bone defect model (Table I). This study provides an in-depth understanding of the local pharmacokinetics of SAPAE treatment and its physiological mechanisms on enhanced diabetic bone formation. Local SA concentration in the bone defect, *in vivo* inflammation, osteoblast and osteoclast density and activities were investigated, which are crucial for a deeper understanding and clinical translation of the previous work.

Previous studies on SAPAE pharmacokinetics only focused on systemic SA release, namely SA released in bulk media.[13] In the rat mandibular bone defect model, however, the local SA concentration within defect is more therapeutically relevant, as it has more direct effects on bone regeneration than systemic SA concentrations. The novel agar-based system presented herein mimics the *in vivo* physical environment of a mandibular bone defect to more accurately model local SA concentrations. The localized yet low SA concentrations at the early stage may allow sufficient early inflammation to occur after injury to initiate the healing cascade.[27] At days 3–6, higher levels of localized SA were detected [Fig. 3(A)], which can help resolve the high level of inflammation that persists in diabetic animals and may hinder bone formation.[28] After 1 week, consistently low levels of local SA (~0.5 mg mL^{-1}) that is comparable to its IC50 (5 μg mL^{-1} to 20 mg mL^{-1}) were released,[21] which could ameliorate the chronic inflammation impairing bone healing in diabetic animal.[29]

The bulk SA release profile was similar to the previous study,[13] where an initial lag period was followed by sustained SA release. However, the agar-based system showed a much longer release duration (60% cumulative release at day 31) compared to the previous study (100% release at day 16), in which a mixture of SAPAE, bone allograft and mineral oil was directly placed in PBS without the shielding of agar.[13] As the effects of SAPAE treatment on inflammation was clearly evident at 28 days *in vivo* (Figs. 5 and 6), the SA release profile shown by the agar-based system is a more relevant model compared to the bulk PBS model.

[13] This result indicates that the agar, which mimics the soft tissues covering the bone defect, significantly hindered SA transport, delayed SA diffusion and ultimately delay polymer degradation. Even though biological factors, such as cells and enzymes, are not included in this model for the sake of simplicity, this study demonstrated that the agar system is an improvement over the bulk PBS model. In addition, this model can be easily expanded to evaluate other drug delivery systems for similar animal models.

The result of prolonged SA release is clearly reflected in inflammation level changes. Animals receiving SAPAE treatments had significantly reduced local inflammation at the defect compared to their non-SAPAE counterparts. This result was demonstrated both at the cellular level (PMN and MNC counts, Fig. 5) and the molecular level (inflammatory marker IL-1α stains, Fig. 6). SAPAE reduced inflammation to a larger extent in diabetic rats, likely due to their already elevated inflammation, which is typical of diabetic humans and animals following an injury. As a result, SAPAE had more prominent effects on other inflammation-relevant responses in diabetic rats, such as osteoclastogenesis and osteoblastogenesis.[30]

Osteoclastogenesis and osteoclast activities, which are directly related to bone resorption, can be overly exacerbated by diabetes-enhanced inflammation during remodeling.[31] This phenomenon is shown in our results as well (Fig. 8). As a result, Animals with reduced inflammation due to SAPAE treatments had significantly lower osteoclasts density and activity compared to their non-SAPAE counterparts, which would result in less bone resorption. Increased inflammation in diabetic animals has also been shown to significantly contribute to reduced bone formation and activity of osteoblasts.[32] This result agrees with our results data showing that diabetic animals without SAPAE have lower osteoblast density than their normoglycemic counterpart (Fig. 9). Our results showed that SAPAE, by suppressing the prolonged inflammation in diabetic rats, normalized the deficit in diabetic bone healing by restoring osteoblast density to the normal level as no significant differences were observed between “diabetic + SAPAE” and “normal + SAPAE” ($P > 0.05$) (Fig. 9). The effect of SAPAE is more prominent in diabetic animals as shown by the significant difference between the SAPAE and non-SAPAE groups even at 12 weeks post-operation (Figs. 8 and 9). Although it has been reported that excessive reduction in osteoclast impairs osteoblastogenesis,[33] the reduced osteoclast density herein did not reduce osteoblastogenesis. This is likely because the continuously low dose of SAPAE mainly normalizes the healing condition in diabetic rats, rather than drastically reducing osteoclastogenesis and distorting the cellular balance.

SAPAE is advantageous as it is purely synthetic and therefore could be easier to acquire than allografts. The degradable SAPAE material does not need secondary surgeries as required by autografts and stem cell-based treatments.[34] SAPAE can be applied at the time of treatment, does not require patient compliance, and is very effective even under poor glucose control. This treatment is significant because diabetic patients are frequently not in full compliance and exhibit a range of glycemic control. SAPAE treatments should be relatively inexpensive compared to growth factors as its raw materials are relatively cheap and the synthetic procedures are relatively straight-forward. While this study focused on bone regeneration using SAPAE powder, SAPAE-based systems could be advantageous for many other applications: SAPAE porous scaffolds for improved vascularization and cell growth; drug-

encapsulating SAPAE microspheres for synergistic, dual drug delivery; and SAPAE hydrogels that simulate extra cellular matrix. While such formulations have been pursued with other polymers such as PLGA and PCL,[35] SAPAE formulations offer the unique advantages of exceedingly high SA loading and well controlled local SA release profiles.

CONCLUSIONS

This study investigated the local pharmacokinetics of SAPAE using a novel agar-based system and evaluated the cellular and molecular mechanisms of localized and sustained SA release on diabetic bone regeneration. With the agar system, a continuous and slow localized release of SA was observed for more than a month; this data correlates with the prolonged local anti-inflammatory effect observed *in vivo*, as demonstrated by histological analysis. The prolonged inflammation mitigation down-regulated osteoclast density and activity, and increased osteoblastogenesis, particularly in diabetic animals.[30,36] As a result, SAPAE significantly enhanced bone formation, especially in diabetic animals.[13]

This study proves that SAPAE treatment enhances diabetic bone formation through prolonged inflammation mitigation. The SA release profile presented herein serves as a reference for future designs of anti-inflammatory treatment for diabetic bone healing; specifically, an initial lag period of ~2 days of low SA concentrations followed by a slow and prolonged SA release for at least 1 month. Future studies will incorporate other osteogenic formulations to further improve system performance, such as utilizing porous scaffold and/or the addition of insulin for diabetic bone regeneration.

Supplementary Material

Refer to Web version on PubMed Central for supplementary material.

ACKNOWLEDGMENTS

The authors thank Dr. Yan Yan and Sandrine Barakat for assistance in preparing part of the histology samples.

Contract grant sponsor: NIH; contract grant numbers: R01AR060055, R01DE-017732, R01 DE13207, R44AA020163

REFERENCES

1. Control CoD. National Diabetes Statistics Report, 2014 2014 http://www.cdc.gov/diabetes/pubs/statsreport14/national-diabetes-report-web.pdf.
2. Boyle JP, Thompson TJ, Gregg EW, Barker LE, Williamson DF. Projection of the year 2050 burden of diabetes in the US adult population: Dynamic modeling of incidence, mortality, and pre-diabetes prevalence. Population Health Metrics 2010;8:29. [PubMed: 20969750]
3. Chaudhary SB, Liporace FA, Gandhi A, Donley BG, Pinzur MS, Lin SS. Complications of ankle fracture in patients with diabetes. J Am Acad Orthopaed Surg 2008;16:159–170.
4. Lu H, Kraut D, Gerstenfeld LC, Graves DT. Diabetes interferes with the bone formation by affecting the expression of transcription factors that regulate osteoblast differentiation. Endocrinology 2003;144:346–352. [PubMed: 12488363]
5. Wu YY, Xiao E, Graves DT. Diabetes mellitus related bone metabolism and periodontal disease. Int J Oral Sci 2015;7:63–72. [PubMed: 25857702]

6. Ko KI, Coimbra LS, Tian C, Alblowi J, Kayal RA, Einhorn TA, Gerstenfeld LC, Pignolo RJ, Graves DT. Diabetes reduces mesenchymal stem cells in fracture healing through a TNFα-mediated mechanism. Diabetologia 2015;58:633–642. [PubMed: 25563724]
7. Alblowi J, Kayal RA, Siqueira M, McKenzie E, Krothapalli N, McLean J, Conn J, Nikolajczyk B, Einhorn TA, Gerstenfeld L, Graves DT. High levels of tumor necrosis factor-alpha contribute to accelerated loss of cartilage in diabetic fracture healing. Am J Pathol 2009;175:1574–1585. [PubMed: 19745063]
8. Retzepi M, Lewis MP, Donos N. Effect of diabetes and metabolic control on de novo bone formation following guided bone regeneration. Clin Oral Implants Res 2010;21:71–79. [PubMed: 19922493]
9. Ramanujam CL, Facaros Z, Zgonis T. An overview of bone grafting techniques for the diabetic charcot foot and ankle. Clin Paediatric Med Surg 2012;29:589.
10. White AP, Vaccaro AR, Hall JA, Whang PG, Friel BC, McKee MD. Clinical applications of BMP-7/OP-1 in fractures, nonunions and spinal fusion. Int Orthopaed 2007;31:735–741.
11. Govender PV, Rampersaud YR, Rickards L, Fehlings MG. Use of osteogenic protein-1 in spinal fusion: Literature review and preliminary results in a prospective series of high-risk cases. Neurosurg Focus 2002;13:1–6.
12. Garrison KR, Donell S, Ryder J, Shemilt I, Mugford M, Harvey I, Song F. Clinical effectiveness and cost-effectiveness of bone morphogenetic proteins non-healing of fractures and spinal fusion: A systematic review 2007;11:1–150.
13. Wada K, Yu W, Elazizi M, Barakat S, Ouimet MA, Rosario-Meléndez R, Fiorellini JP, Graves DT, Uhrich KE. Locally delivered salicylic acid from a poly(anhydride-ester) impact on diabetic bone regeneration. J Controlled Release Off J Controlled Release Soc 2013;171:33–37.
14. Ji J, Hao S, Wu D, Huang R, Xu Y. Preparation, characterization and in vitro release of chitosan nanoparticles loaded with gentamicin and salicylic acid. Carbohydr Polym 2011;85:803–808.
15. Ouimet MA, Snyder SS, Uhrich KE. Tunable drug release profiles from salicylate-based poly(anhydride-ester) matrices using small molecule admixtures. J Bioact Compat Polym 2012;27: 540–549. [PubMed: 24078768]
16. McCarty MF, Block KI. Preadministration of high-dose salicylates, suppressors of NF-kappaB activation, may increase the chemosensitivity of many cancers: An example of proapoptotic signal modulation therapy. Integr Cancer Ther 2006;5:252–268. [PubMed: 16880431]
17. Housby JN, Cahill CM, Chu B, Prevelige R, Bickford K, Stevenson MA, Calderwood SK. Non-steroidal anti-inflammatory drugs inhibit the expression of cytokines and induce HSP70 in human monocytes. Cytokine 1999;11:347–358. [PubMed: 10328874]
18. Pfeilschifter J, Chenu C, Bird A, Mundy GR, Roodman DG. Interleukin-1 and tumor necrosis factor stimulate the formation of human osteoclastlike cells in vitro. J Bone Miner Res 1989;4:113–118. [PubMed: 2785743]
19. Elavarasu S, Sekar S, Murugan T. Host modulation by therapeutic agents. J Pharm Bioallied Sci 2012;4:S256–S259. [PubMed: 23066265]
20. Roszer T. Inflammation as death or life signal in diabetic fracture healing. Inflamm Res Off J Eur Histamine Res Soc 2011;60:3–10.
21. Panda H Handbook on Drugs from Natural Sources. India: Asia Pacific Business Press Inc; 2010.
22. Kini U, Nandeesh B. Physiology of Bone Formation, Remodeling, and Metabolism. Radionuclide and Hybrid Bone Imaging. Germany: Springer; 2012 p 29–57.
23. Pacios S, Andriankaja O, Kang J, Alnammary M, Bae J, de Brito Bezerra B, Schreiner H, Fine DH, Graves DT. Bacterial infection increases periodontal bone loss in diabetic rats through enhanced apoptosis. Am J Pathol 2013;183:1928–1935. [PubMed: 24113454]
24. Kang J, de Brito Bezerra B, Pacios S, Andriankaja O, Li Y, Tsiagbe V, Schreiner H, Fine DH, Graves DT. Aggregatibacter actinomycetemcomitans infection enhances apoptosis in vivo through a caspase-3-dependent mechanism in experimental periodontitis. Infect Immun 2012;80:2247–2256. [PubMed: 22451521]
25. Everts V, Delaissé JM, Korper W, Jansen DC, Tigchelaar-Gutter W, Saftig P, Beertsen W. The bone lining cell: Its role in cleaning Howship's lacunae and initiating bone formation. J Bone Miner Res 2002;17:77–90. [PubMed: 11771672]

26. Bezerra Bde B, Andriankaja O, Kang J, Pacios S, Bae HJ, Li Y, Tsiagbe V, Schreiner H, Fine DH, Graves DT. A. actinomycetemcomitans-induced periodontal disease promotes systemic and local responses in rat periodontium. J Clin Periodontol 2012;39:333–341. [PubMed: 22313458]
27. Simmons DJ. Fracture healing perspectives. Clin Orthop Relat Res 1985;200:100–113.
28. Zhang X, Kohli M, Zhou Q, Graves DT, Amar S. Short-and long-term effects of IL-1 and TNF antagonists on periodontal wound healing. J Immunol 2004;173:3514–3523. [PubMed: 15322216]
29. Ouimet MA, Fogaca R, Snyder SS, Sathaye S, Catalani LH, Pochan DJ, Uhrich KE. Poly(anhydride-ester) and poly(N-vinyl-2-pyrrolidone) blends: salicylic acid-releasing blends with hydrogel-like properties that reduce inflammation. Macromol Biosci 2015;15: 342–350. [PubMed: 25333420]
30. Mountziaris PM, Spicer PP, Kasper FK, Mikos AG. Harnessing and modulating inflammation in strategies for bone regeneration. Tissue Eng B Rev 2011;17:393–402.
31. Liu R, Bal HS, Desta T, Krothapalli N, Alyassi M, Luan Q, Graves DT. Diabetes enhances periodontal bone loss through enhanced resorption and diminished bone formation. J Dental Res 2006;85:510–514.
32. Pacios S, Kang J, Galicia J, Gluck K, Patel H, Ovaydi-Mandel A, Petrov S, Alawi F, Graves DT. Diabetes aggravates periodontitis by limiting repair through enhanced inflammation. FASEB J Off Publ Feder Am Soc Exp Biol 2012;26:1423–1430.
33. Matsuo K, Irie N. Osteoclast–osteoblast communication. Arch Biochem Biophys 2008;473:201–209. [PubMed: 18406338]
34. Paleev NR, Odinokova VA, Gurevich MA, Mravian SR, Borisov Iu P, Bronnikov SM, Obrezkov GV. Correlation analysis of hemodynamic and morphological parameters in patients with myocarditis. Kardiologiia 1989;29:72–75.
35. Zhang HX, Xiao GY, Wang X, Dong ZG, Ma ZY, Li L, Li YH, Pan X, Nie L. Biocompatibility and osteogenesis of calcium phosphate composite scaffolds containing simvastatin-loaded PLGA microspheres for bone tissue engineering. J Biomed Mater Res A 2015;103:3250–3258. [PubMed: 25809455]
36. Mountziaris PM, Mikos AG. Modulation of the inflammatory response for enhanced bone tissue regeneration. Tissue Eng B Rev 2008;14:179–186.

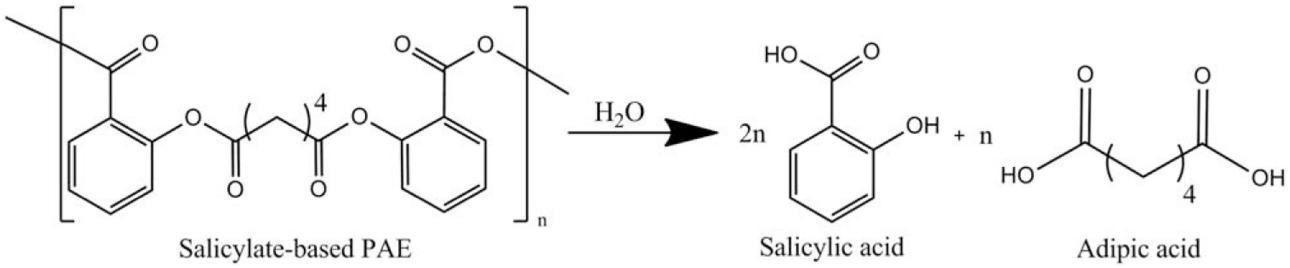

FIGURE 1.
SAPAE degradation releases SA and adipic acid upon anhydride and ester bond hydrolysis.

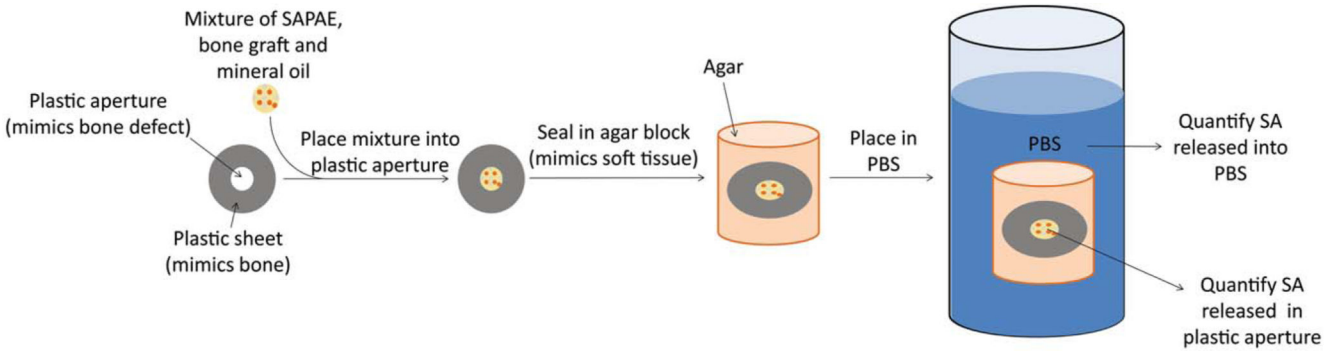

FIGURE 2.

Schematic representation of the agar-based system that mimics the animal model *in vivo* environments. Mixtures containing SAPAE were placed within the plastic aperture, then sealed in an agar block. This system mimics the physical environments of the mandibular bone defect and the surrounding soft tissues.

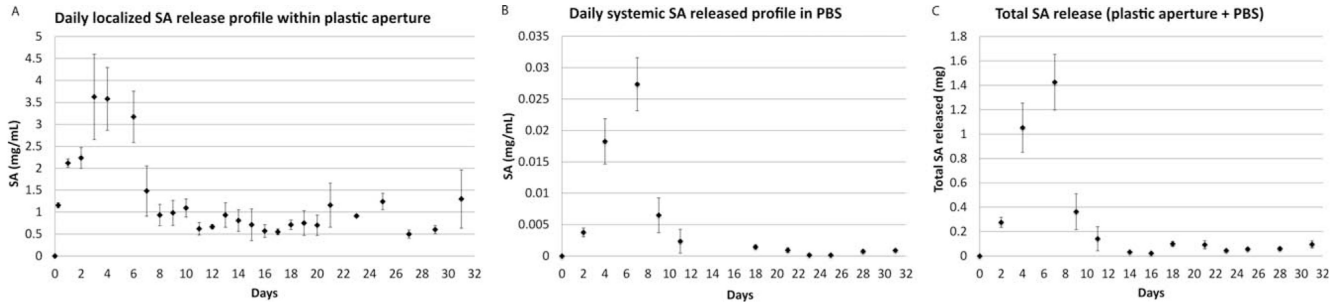

FIGURE 3.

(A) SA washed from samples within the plastic aperture; (B) SA released into the PBS phase (blue region as indicated in cartoon of Fig. 2) and (C) total amount of SA released from SAPAE at each time point (plastic aperture plus PBS) (N = 3, mean ± standard deviation).

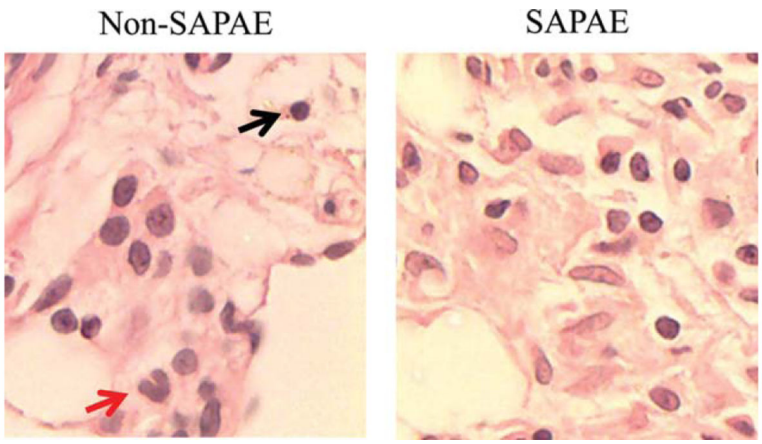

FIGURE 4.

Representative micrographs of PMN (with a horse-shoe shape nucleus, indicated by red arrow) and MNC (with a round and dark nucleus, indicated by black arrow) in diabetic animals with and without SAPAE treatment. Pictures were taken under ×60 objective. Cells with similar morphology were identified as PMNs and MNCs for all specimens.

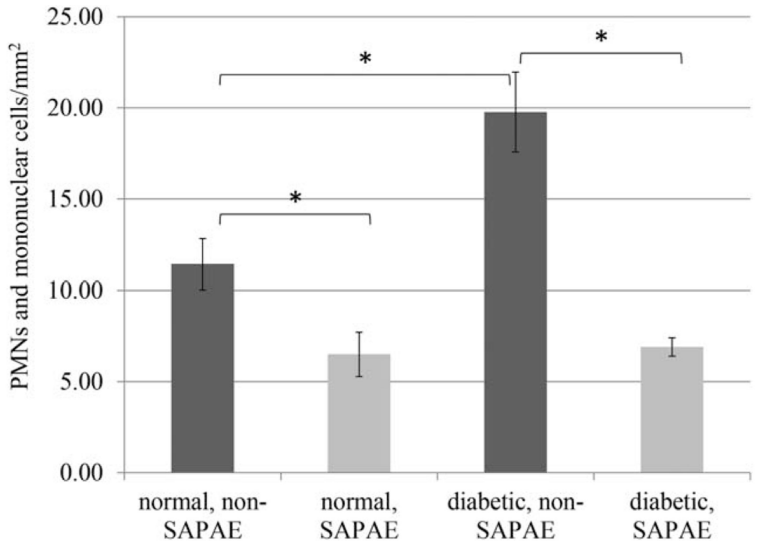

FIGURE 5.

PMNs and mononuclear cells per mm^2 in area of new bone formation at 4 weeks. SAPAE significantly reduced inflammatory cells, especially in diabetic rats. $N = 5–8$ per group and data presented as mean ± standard error; * indicates $P < 0.05$.

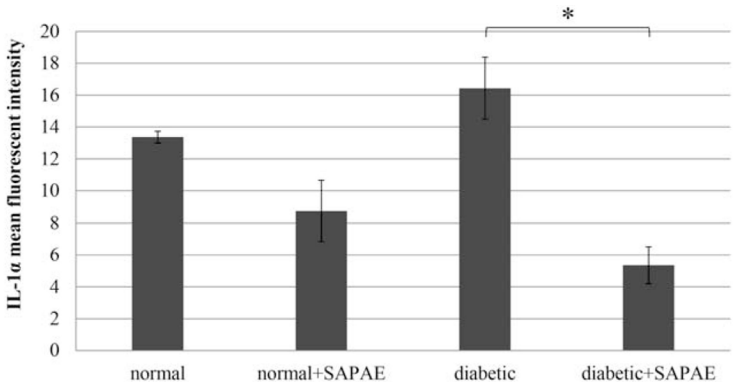

FIGURE 6.

Mean fluorescent intensity of IL-1α in area of new bone formation at 4 weeks, indicating inflammation level. SAPAE significantly reduced IL-1α level in diabetic rats. $N = 4–6$ per group and data presented as mean ± standard error; * indicates $P < 0.05$.

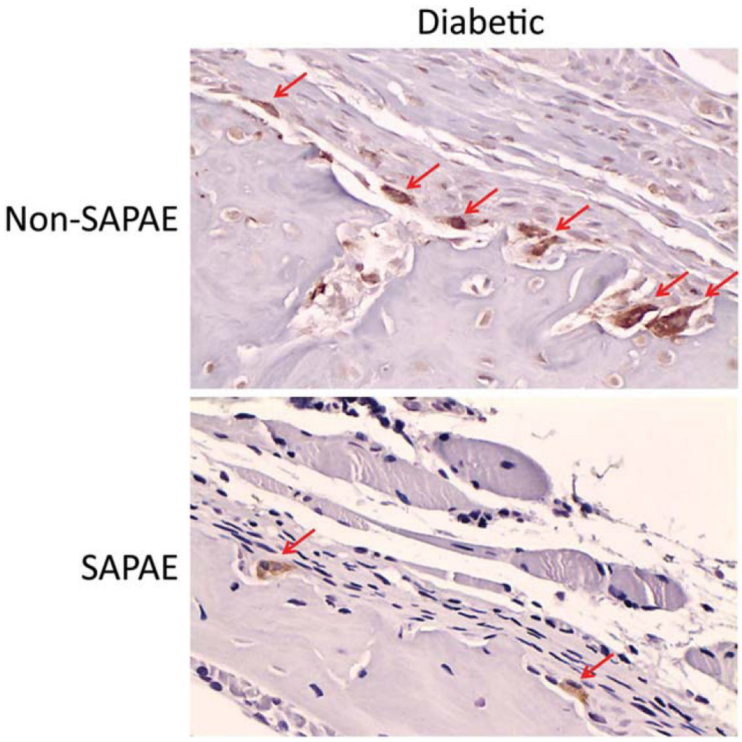

FIGURE 7.
Representative images of bone lining osteoclasts in each group. Pictures taken under ×10 objective.

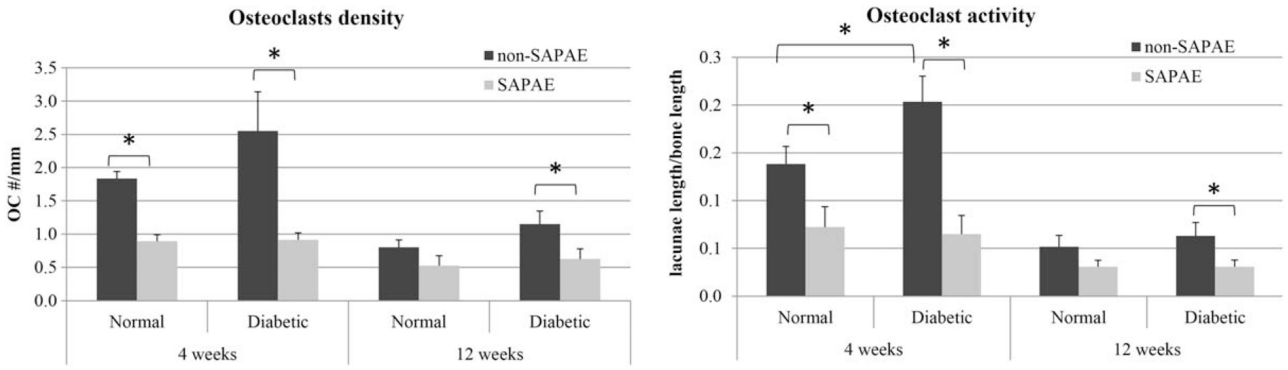

FIGURE 8.

(Left) Bone-lining osteoclast density and (right) osteoclast activity indicated by the portion of bone surface occupied by lacunae within the area of new bone formation. SAPAE significantly reduced osteoclast activity and density in normal rats at 4 weeks and in diabetic rats at both 4 and 12 weeks. $N = 5–8$ per group and data presented as mean ± SD; * indicates $P < 0.05$.

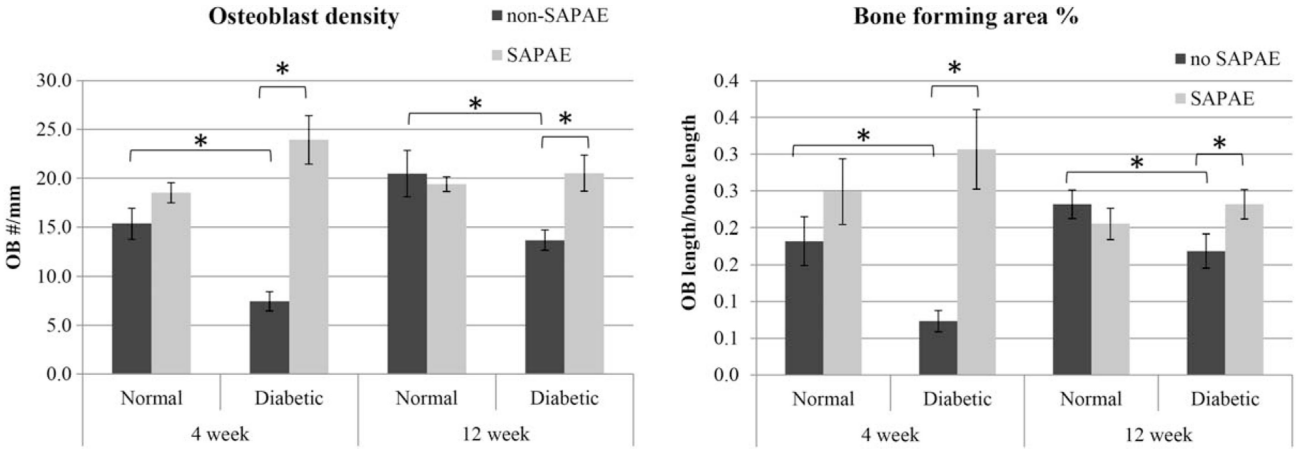

FIGURE 9.

(Left) Bone-lining osteoblast density and (right) the percentage of bone forming area within ROI, indicated by the percentage of bone surface covered by osteoblasts. SAPAE significantly increased osteoblast density and bone forming area in diabetic rats at both 4 and 12 weeks. $N = 5–8$ per group and data presented as mean ± standard error; * indicates $P < 0.05$.

Author Manuscript

Author Manuscript

Author Manuscript

TABLE I.

Relative Ratio of Bone Regeneration with SAPAE Treatment Over Control ($N = 6$)

	4 Weeks		12 Weeks	
	Diabetic	**Normal**	**Diabetic**	**Normal**
Mean ± Std	1.36 ± 0.21	1.40 ± 0.32	1.45 ± 0.25	1.17 ± 0.24